Jul 1st, 12:00 AM

# Spatial modelling of potential soil water retention under floodplain inundation using remote sensing and GIS

Yun Chen

Bing Wang

C. A. Pollino

Linda Merrin

*International Environmental Modelling and Software Society (iEMSs)*
*2012 International Congress on Environmental Modelling and Software*
*Managing Resources of a Limited Planet, Sixth Biennial Meeting, Leipzig, Germany*
*R. Seppelt, A.A. Voinov, S. Lange, D. Bankamp (Eds.)*
*http://www.iemss.org/society/index.php/iemss-2012-proceedings*

# Spatial modelling of potential soil water retention under floodplain inundation using remote sensing and GIS

**Yun Chen*, Bing Wang, Carmel Pollino, Linda Merrin**
*CSIRO Land and Water, Canberra, Australia (yun.chen@csiro.au)*

**Abstract:** Flood inundation and retention are key hydrological characteristics of floodplain wetlands. They are critical to the management of environmental flows in terms of sustaining ecosystem function, biodiversity and habitat suitability. This study developed a methodology for the estimate of potential floodwater retention under floodplain inundation from ecologically significant flood return periods by coupling remote sensing and GIS technologies with spatial hydrological modelling. The Macquarie Mashes located in the central west of New South Wales of Australia were selected as the case study area. The 1-in-10 years annual recurrence interval (ARI) was identified as one of the most important return periods to be investigated. A partial duration flood frequency analysis was applied to time series of observed flow data for generating a return period curve (RPC). Time-series of MODIS 8-day composite imagery (500m resolution) over the period 2000-2011 were related to the 1-in-10 ARI flow rate (ML/day) quantified from the RPC. Inundation in each corresponding image was detected using the modified Normalised Difference Water Index (mNDWI) in ENVI. The potential maximum retention was measured using a spatial hydrological modelling approach, which is driven by the Soil Conservation Service Curve Number (SCS CN) method. Soil and land cover data were collected and intersected to determine spatial distribution of CN in ArcGIS. The resultant retention capacity map was then integrated with inundation extent map to delineate the spatial pattern of potential retention under inundation which has ecological implications in the study area. This study has proved that the integration of remote sensing, GIS and spatial hydrologic modelling can be used to provide essential information as inputs to environmental models for understanding the responses of floodplain and wetland ecosystems and to support the assessment of the benefits of returning water to these environments.

***Keywords**:* Wetland; OWL; mNDWI; MODIS; TM; CN

## 1 INTRODUCTION

Retention of water in a wetland or in depressions of a floodplain contributes to meeting the needs of function, biodiversity and habitat suitability in river systems. Environmental water requirements are often expressed as the extent, duration and frequency of inundation events. Without a greater understanding of retention of water after an event, the flows required to meet duration requirements for meeting ecological requirement can be poorly estimated. Therefore, the mapping of the retention associated with the inundation events is crucial to improving the flows required to meet environmental water requirements of floodplain wetlands.

In recent years there is a growing interest in developing techniques for the evaluation and rehabilitation of the ecological health of semi-arid floodplain wetlands, many of which are being lost or threatened due to increasing demands of water for irrigation (Lemly et al., 2000). Many studies have investigated either the modelling of inundation extent or methods of retention estimate (Horritt and Bates,

2002; Romanowicz and Beven, 2003; Noe and Hupp, 2007; Valentova et al., 2010). For ecological studies, these methods need to account for the relationships between flow and ecological response, either implicitly or explicitly. Advances in remote sensing and Geographic Information Systems (GIS) have provided a decisive and effective tool for enhancing spatial eco-hydrological modelling. These technologies have been actively explored in numerous areas, such as flood monitoring, prediction or forecasting (Usachev, 1987; Barton and Bathols, 1989; Prigent et al., 2001; Wang et al., 2002; Frazier et al., 2003; Knebl et al., 2005), flood risk assessment or evaluation (Smith, 1997; Islam and Kimiteru, 2000; Liu et al., 2002) and potential retention estimation (Saito et al., 2009). However, few studies have examined the integration of spatial modelling of floodplain inundation extent and the estimate of floodwater retention under inundation. Much less is known about linking floodplain inundation corresponding to flood return periods which are ecologically meaningful to the delineation of spatial variation of the retention capacity. Therefore, here we present a preliminary study designed to demonstrate the capability of coupling remote sensing and GIS with spatial hydrological modelling to estimate potential floodwater retention under floodplain inundation relevant to ecologically significant flood return periods, in terms of annual recurrence intervals (ARIs).

The Macquarie Marshes, located in the central west of New South Wales, Australia, were selected as the case study for this paper (Figure 1). The Marshes are an extensive, semi-permanent inland wetland system which has a network of interconnecting channels, lagoons, effluents and associated overflow areas. The study site covers about 1,360,000 hectares (Ha). The wetlands are characterised by the layer of fresh water essentially fed by rainfall and the Macquarie River without groundwater recharge (Macaulay and Kellett, 2009). The area of the wetlands depends on water availability and extends to about 300,000 hectares during major floods (Thomas et al., 2011). The mean annual rainfall and the evaporation rate in the Macquarie Marshes are 432 mm (Paijmans, 1981) and 1800 mm (DWR, 1991), respectively. Average temperatures vary from a daily minimum of 4oC during winter months to a daily maximum of 35oC during summer (Kingsford and Thomas, 1995). Listed in 1986 as a Wetland of International Importance under the Ramsar Convention, the Marshes are a well-known habitat of waterbirds, are an important refuge for a large number of other wildlife species and have significant cultural values. The patterns of flooding and water dependent vegetation produced by rivers and streams in and around the Marshes are of particular importance to this study.

## 2 ESTIMATE OF INUNDATION EXTENT - FLOODPLAIN INUNDATION MODELLING

### 2.1 Determination of ARI Flow from Flood Frequency Analysis

A flood return period, or ARI, is the average number of years between floods of a certain size. The 1-in-10 ARI flow stands for a statistically estimated magnitude of flow that occurs once every 10 years, which was identified as being an ecologically

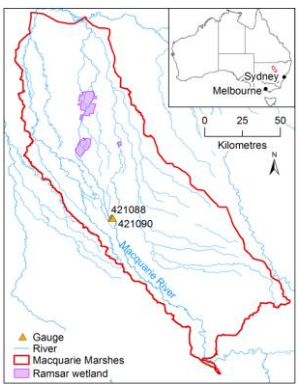


**Figure 1.** Macquarie Marshes and its surrounding area.

significant event, meeting the majority of environmental water requirements across the entirety of the Macquarie Marshes. This ARI flow was quantified from the observed daily flow time series data (ML/day), collected from the gauging stations (Figure 1) just upstream of the main wetland complex. It was derived using a return period curve (RPC), which was generated using the flood frequency analysis in the River Analysis Package (eWater CRC, 2012). The 1-in-10 ARI flow in the study area was determined to be 7180 ML/day.

### 2.2 Derivation of Inundation from Remotely Sensed Imagery

Time-series of MODIS (Moderate Resolution Imaging Spectroradiometer) of 500m 8-day surface reflectance imagery (MOD09A1 collection 5; USGS, 2010) were acquired over the period 2000-2011. Inundation in each image was detected using the modified Normalised Difference Water Index (mNDWI, Xu 2006) which was developed based on a combination of reflectance in the green and shortwave-infrared wavelengths. The mNDWI is calculated as in Equation 1:

$$mNDWI = \frac{Band\ 4 - Band\ 6}{Band\ 4 + Band\ 6} \quad (1)$$

where *Band* 4 and Band 6 are reflectance in MODIS bands 4 and 6, respectively. mNDWI pixel values range from -1 to 1. The spatial distributions of the mNDWI were evaluated using 30m resolution Landsat5 TM images to determine the cut-off points for distinguish water bodies and inundated areas. mNDWI pixel values greater than 0 represent permanent water. A threshold of mNDWI values between -0.45 and zero was used to indicate inundation. A 3 x 3 filter was then used to integrate the pixels with a large number of small-scattered pixels. Some examples of processed mNDWI images are given in Figure 2a and Figure 2b.

### 2.3 Spatial Modelling of Inundation Extent

This study assumed that the maximum inundation extent for the 1-in-10 ARI was caused by flood peak discharges, where a peak flow was considered as the maximum flow within a ± 65 day interval in daily flow time series for the observation gauge. Peak flows (mean discharge - ML/day) occurred during the period of MODIS imagery acquisition were extracted from the observed flow time series (Table 1). The dates of the peak flow events were used to select contemporaneous MODIS images. A series of mNDWI derived inundation extents that were concurrent with the flow events of size similar to the ARI flow rate were then mapped. The following rules were also applied taking into account flood duration and the uncertainties in both observed flow records and ARI flow determination:

- based on the date of each 1-in-10 peak flow event, four mNDWI images from before (one scene), during (one scene) and after (two scenes) were joined to represent the inundation extent of that peak flow; and
- all mNDWI inundation extents associated with a peak flow event between 90% and 110% (or within the range of ± 10%) of the 1-in-10 ARI flow rate were combined, by taking the MAXIMUM mNDWI value for each cell/pixel.

A final map (Figure 2c) showing the potential maximum inundation extent for the 1-in-10 ARI was generated by merging the boundary on each of the eight images listed in Table 1.

**Table 1.** The 1-in-10 ARI flow defined from flood frequency analysis and corresponding peak flows extracted from observed flow time series.

| ARI | ARI Flow (ML/day) | ± 10% ARI Flow (ML/day) | Observed Peak Flow (ML/day) | Peak Date | MODIS image |
|---|---|---|---|---|---|
| 1-in-10 | 7180 | 6462-7898 | 7441 | 30/11/2000 | 329/337/345/353 |
| | | | 7300 | 15/12/2010 | 345/353/361/001 |

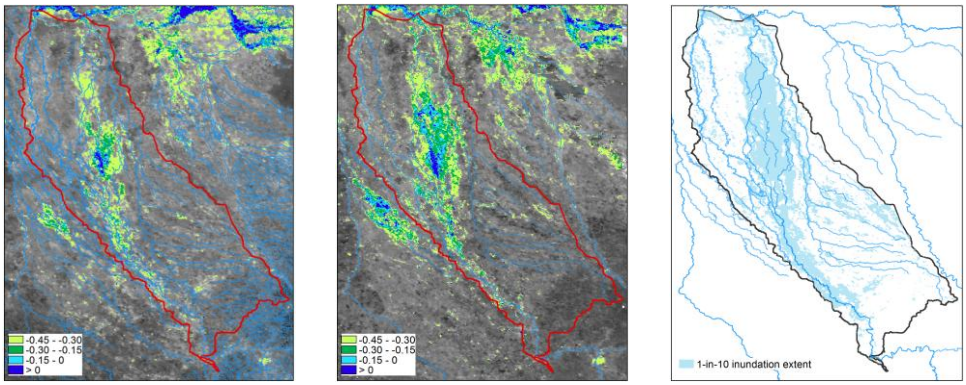


(a) (b) (c)

**Figure 2.** (a) and (b) Examples of MODIS 8-days composite mNDWI images representing inundation extent for the 1-in-10 ARI events from 02/12/2000 to 09/12/2000 and from 19/12/2010 to 26/12/2010, respectively; (c) Final inundation extent map for the 1-in-10 ARI.

## 3 ESTIMATE OF FLOOD RETENTION – SPATIAL HYDROLOGICAL MODELLING

The potential floodwater retention is defined as potential maximum soil water retention (PMSWR) in this study. The PMSWR was modelled using a spatial hydrological modelling approach, which is driven by the Soil Conservation Service Curve Number (SCS CN) method. The geospatial hydrology toolkit, HEC-GeoHMS (Hydrologic Engineering Centre's Geo-Hydrologic Modelling System), was employed for this purpose (Fleming and Doan, 2009). Details are discussed in the following sections.

### 3.1 Curve Numbers

The curve number method was developed by the USDA Natural Resources Conservation Service, which was formerly called the Soil Conservation Service. The number is still popularly known as a "SCS CN" which is an empirical parameter used in hydrology for predicting direct runoff or infiltration from rainfall excess (McCuen, 1982).

Determination of CN depends on the soil hydrologic characteristics and ground cover conditions in the watershed. The main drivers of CN are the hydrologic soil group (HSG) and cover type. HSG reflects infiltration rates of soils, which are classified as four groups, A, B, C and D. Group A has the highest infiltration rate (lowest CN with more sands and gravels) and Group D has the lowest infiltration rate (highest CN with more silts and clays). References, such as from SCS (1986), indicate the CN values for possible land cover and HSG combinations.

Soils and land cover data were obtained from the Digital Atlas of Australian Soils at a scale of 1:2,000,000 and the National Vegetation Information System (NVIS) with a 100m x100m cell size, respectively. Ground cover in the study area was classified into 23 cover types (Table 2). Soils are grouped into four HSGs. The cover and HSG data were intersected in the HEC-GeoHMS to generate a new data layer which contains each individual cell (500m x500m) with a unique combination of HSG and land cover features. A CN value was then assigned to each cell using the lookup table (Table 2) to derive a raster CN distribution map (Figure 3a).

CN under the different land cover and soil features in the study area are summarised in Table 2, ranging from 30 to 94. Lower numbers indicate low runoff

**Table 2.** Simplified CN lookup table for the study area based on the list published in TR-55 Manual (SCS, 1986).

| COVER CLASS | CN for HSG | | | |
|---|---|---|---|---|
| | A | B | C | D |
| Eucalyptus open forests with a shrubby understorey | 30 | 55 | 70 | 77 |
| Eucalyptus woodlands with a shrubby understorey | 30 | 55 | 70 | 77 |
| Callitris forests and woodlands | 30 | 55 | 70 | 77 |
| Brigalow (Acacia harpophylla) forests and woodlands | 30 | 55 | 70 | 77 |
| Other Acacia forests and woodlands | 30 | 55 | 70 | 77 |
| Other forests and woodlands | 30 | 55 | 70 | 77 |
| Casuarina and Allocasuarina forests and woodlands | 30 | 55 | 70 | 77 |
| Eucalyptus open forests with a grassy understorey | 36 | 60 | 73 | 79 |
| Eucalyptus woodlands with a grassy understorey | 36 | 60 | 73 | 79 |
| Eucalyptus open woodlands with shrubby understorey | 36 | 60 | 73 | 79 |
| Mallee with hummock grass | 32 | 58 | 72 | 79 |
| Eucalyptus open woodlands with a grassy understorey | 32 | 58 | 72 | 79 |
| Arid and semi-arid acacia low open woodlands and shrublands with chenopods | 43 | 65 | 76 | 82 |
| Eucalyptus low open woodlands with a shrubby understorey | 43 | 65 | 76 | 82 |
| Eucalyptus low open woodlands with a chenopod or samphire understorey | 43 | 65 | 76 | 82 |
| Saltbush and Bluebush shrublands | 35 | 56 | 70 | 77 |
| Other shrublands | 35 | 56 | 70 | 77 |
| Other tussock grasslands | 49 | 69 | 79 | 84 |
| Wet tussock grassland with herbs, sedges or rushes, herblands or ferns | 49 | 69 | 79 | 84 |
| Sedgelands, rushs or reeds | 49 | 69 | 79 | 84 |
| Mixed chenopod, samphire +/- forbs | 38 | 63 | 74 | 80 |
| Naturally bare, sand, rock, claypan, mudflat | 77 | 86 | 91 | 94 |
| Cleared, non-native vegetation, buildings | 48 | 66 | 78 | 83 |

potential, whilst larger numbers indicate an increase in runoff potential. In other words, the lower the CN, the more permeable the soil.

### 3.2 Estimate Flood Retention

Based on the SCS CN method, the PMSWR at cell i ($PMSWR_i$) is parameterised as a function of a CN ($CN_i$) value for the cell. This is given by Equation 2:

$$PMSWR_i = PMSWR_0 \left(\frac{100}{CN_i} - 1\right) \quad (2)$$

where $0 < CN_i < 100$, and $PMSWR_0$ is a scale factor depending upon the unit used, e.g. $PMSWR_0 = 10$ for units of inches, and $PMSWR_0 = 254$ for units of millimetres. $PMSWR_i$ was calculated cell by cell within the HEC-GeoHMS. It is obvious that the estimate of PMSWR is related to the soils and cover conditions of the study area through CN which depends on land cover and HSG in the study area. Figure 3b is the resultant PMSWR map in the study area.

## 4 RESULTAS AND DISCUSSIONS

The total area of inundation for a 1-in-10 year return period was calculated from Figure 2c. There are about 437,000 Ha being inundated, which is about 32% of the total study area and covers almost the whole Marshes wetland area. The inundation extent was overlaid on the vegetation map. The results can be inferred that, within the areas inundated by a 1-in-10 ARI flood, about 31% is Eucalyptus woodlands and open forests with a shrubby understory, 7% is other Acacia forests and woodlands distributed in the southwest, 6% is Eucalyptus open woodlands with a grassy understory, and 29% is saltbush and Bluebush shrublands. It has to be noted that the above statistics were largely driven by inundation extent estimated using MODIS images which have a resolution of 500 m. Results will be different from what has been showed in this study if using data from other sources, such as higher resolution Landsat imagery.

The spatial patterns the PMSWR are mainly determined by the spatial heterogeneousness of land cover (or vegetation) and soils of the inundated areas. The representation of such a combination is the CN value. Therefore, it can be seen from Figure 3a and Figure 3b that the spatial distributions of the CN and PMSWR are similar. The resultant flood retention map (Figure 3b) was overlaid with inundation extent maps (Figure 2c) to delineate the spatial pattern of the retention under inundation of 1-in-10 ARI which has ecological implications in the study area. It is indicated that most inundated area (85% of total) falling in the PMSWR range from 30 to 90mm. About half of inundation extent (49%) confines to the 30 to 60mm retention values, and 36% inundation occur on where PMSWR varies between 60 and 90mm. Only 13% and 2% inundated area have PMSWR values greater than 90mm and smaller the 30mm, respectively. This means that about 85% of the inundated area can retain some soil moisture where some vegetation reliant on relatively frequent flooding may also survive during prolonged dry periods.

The areas with highest soil water retention are those that overlap with vegetation types (Table 2) with a higher water requirement, or wet environment. Eucalypts dominate areas with clay soils, which also have a have a potential for retaining water. Likewise, areas with a lower soil water retention potential overlap with areas where water requirements are lower or environment is dry. This outcome confirms the importance of retention, and soil type, in determining the delivery of flows to meet environmental water requirements in floodplain wetlands.

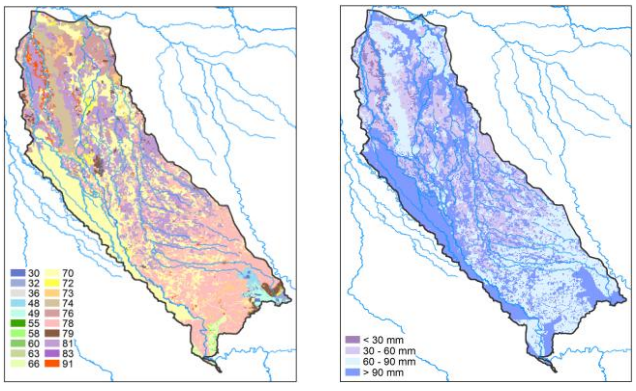


(a) (b)

**Figure 3.** (a) CN distribution derived from the combination of HSG and land cover using the CN lookup table (Table 2); (b) Map of potential maximum soil water retention (PMSWR).

The information extracted from spatial inundation and retention analysis can be used to target specific aims for allocation of environmental water in order to prevent decline of ecological components. These results allow the detection of areas which may be little or much ecological benefit in providing water to stressed vegetation. For example, there is probably no need to provide environmental water on the outer extent of the Marshes where is not inundated by a 1-in-10 year flood; whereas for the area where is inundated and associated with higher retention, it is possible to maximise environmental return through higher priority of environmental watering.

## 5 CONCLUSION

This study developed a methodology for the estimate of potential maximum soil water retention under floodplain inundation from an ecologically significant flood return period by integrating remote sensing and GIS technologies with spatial hydrological modelling. Mapping inundation using MODIS 8-day composite data which have sufficient observation frequency has increased the chance of acquiring relatively cloud free imagery during floods at a regional scale. The approach of linking inundation extent with certain ARIs can be used to highlight and prioritise the areas which may be critical in environmental watering for the restoration of ecosystems. Coupled with powerful spatial algorithms, the merging/fusion of hydrologic modelling with ArcGIS also holds the promise of a cost-effective alternative for regional studies on a grid basis. Retention computed cell by cell provides greater detail than traditional basin average methods. The ability to perform spatial analysis for the development of spatially distributed hydrologic parameters, such as potential soil moisture retention, not only saves time and effort, but also improves accuracy over traditional methods. The integration of these techniques can provide essential information as inputs to environmental models for understanding the responses of floodplain and wetland ecosystems and to support the assessment of the benefits of returning water to these environments. However, CN was used as a single parameter to measure the retention in this trial study regardless the impacts of other factors such as evapotranspiration (ET) which will be considered in an ongoing research.

## ACKNOWLEDGMENTS

We would like to thank Dr Emmanuel Xevi (Murray–Darling Basin Authority, Australia) for his knowledge in soil classification.

## REFERENCES

Barton, I.J., and J.M. Bathols, Monitoring floods with AVHRR, *Remote Sensing of Environment, 30*,89-94, 1989.

DWR (Department of Water Resources), Water Resources of the Castlereagh Macquarie and Bogan Valley, Department of Water Resources NSW: Sydney, 1991.

eWater CRC (Cooperative Research Centre), http://www.toolkit.net.au/Tools/RAP, 2012.

Fleming, M.J., and J.H. Doan, HEC-GeoHMS Geospatial Hydrologic Modelling Extension: User's Manual Version 4.2, US Army Corps of Engineers, Institute for Water Resources, Hydrologic Engineering Centre, Davis, CA, 2009.

Frazier, P., K. Page, J. Louis, S. Briggs, and A.I. Robertson, Relating wetland inundation to river flow using Landsat TM data, *International Journal of Remote Sensing, 24*(19), 3755-3770, 2003.

Horritt, M.S. and P.D. Bates, Evaluation of 1D and 2D numerical models for predicting river flood inundation, *Journal of Hydrology, 268*, 87-99, 2002.

Islam, M. and S. Kimiteru, Flood hazard assessment in Bangladesh using NOAA AVHRR data with GIS, *Hydrological Processes, 14*, 605-620, 2000.

Knebl, M.R., Z.L. Yang, K. Hutchison, and D.R. Maidment, Regional scale flood modelling using NEXRAD, rainfall, GIS and HEC-HMS\RAS: a case study for the Sun Antonio river basin summer 2002 storm event, *Journal of Environmental Management*, *75,* 325-336, 2005.

Kingsford, R. T. and R. F. Thomas, The Macquarie Marshes in arid Australia and their waterbirds: a 50-year history of decline, *Environmental Management, 19*(6), 867-878, 1995.

Lemly, A.D, R.T. Kingsford, and J.R. Thompson, Irrigated agriculture and wildlife conservation: conflict on a global scale, *Environmental Managementj, 25*, 485-512, 2000.

Macaulay, S., and J. Kellett, Mapping groundwater and salinity using airborne electromagnetics in the Lower Macquarie River Valley, New South Wales, Australian Government Bureau of Rural Sciences, 2009.

McCuen, R.H., A Guide to Hydrologic Analysis Using SCS Methods, Prentice-Hall, Inc. Englewood Lliffs, New Jersey, No. 35174, pp. 145, 1982.

Noe, G.B., and C.R. Hupp, Seasonal variation in nutrient retention during inundation of a short-hydroperiod floodplain. *River Research and Application, 23*, 1088-1101, 2007.

Paijmans, K., The Macquarie Marshes of Inland Northern NSW, Research Technical Paper No. 40, Division of Land Use, CSIRO: Canberra, 1981.

Prigen, C., E. Mattews, F. Aires, and W.B Rossow, Remote sensing of global wetland dynamics with multiple satellite data sets, *Geophysical Research letter, 28*, 4631-4634, 2001.

Romanowicz, R.J. and Beven, K. J., 2003. Bayesian estimation of flood inundation probabilities as conditioned on event inundation maps. *Water Resources Research* 39:10731089

Saito, H., K. Seki, and J. Simunek, An alternative deterministic method for the spatial interpolation of water retention parameters, *Hydrology and Earth System Sciences, 13*, 453-465, 2009.

SCS (Soil Conservation Service), Urban Hydrology for Small Watersheds, Technical Release 55 (TR-55), 1986.

Smith, L.C., Satellite remote sensing of river inundation area, stage, and discharge: a review, *Hydrological Processes, 11*, 1427-1439, 1997.

Thomas, R.F., R. T. Kingsford, Y. Lu, and S. Hunter, Landsat mapping of annual inundation (1979-2006) of the Macquarie Marshes in semi-arid Australia, *International Journal of Remote Sensing, 32*(16), 4545-4569, 2011.

Usachev, V.F., Evaluation of floodplain inundations by remote sensing methods, In Hydrological Applications of Remote Sensing and Data Transmission, edited by B.E. Goodisom (Wallingford; International Association of Hydrological Sciences), pp. 475-482, 1985.

USGS, MOD09A1 Product page, United States Geological Service & NASA, Land Process Distributed Active Archive Centre MODIS Product Table, https://lpdaac.usgs.gov/lpdaac/products/modis_products_table/surface_reflectance/8_day_l3_global_500m/mod09a1 (accessed 02.08.10), 2010.

Valentova, J., P. Valenta, and L. Weyskrabova, Assessing the retention capacity of a floodplain using a 2D numerical model, *Journal of Hydrology and Hydromechanics, 58*(4), 221-232, 2010.

Wang, Y., J.D. Colby, and K.A. Mulcahy, An efficient methid for mapping flood extent in a coastal flood plain using Landsat TM and DEM data, *International Journal of Remote Sensing, 23*(18), 3681-3696, 2002.

Xu, H., Modification of normalised difference water index (NDWI) to enhance open water features in remotely sensed imagery, *International Journal of Remote Sensing*, *27*, 3025-3033, 2006.